PCCP

Buckybowls as gas adsorbents: binding of gaseous pollutants and their electric-field induced release

Journal:	*Physical Chemistry Chemical Physics*
Manuscript ID	CP-ART-05-2020-002645.R1
Article Type:	Paper
Date Submitted by the Author:	07-Sep-2020
Complete List of Authors:	Burrill, Daniel; University of Pittsburgh, Chemistry Lambrecht, Daniel; Florida Gulf Coast University, Chemistry and Physics; University of Pittsburgh, Chemistry

Buckybowls as gas adsorbents: binding of gaseous pollutants and their electric-field induced release

Daniel J. Burrill[†] and Daniel S. Lambrecht[*,†,‡]

†*Department of Chemistry, University of Pittsburgh, Pittsburgh, Pennsylvania*

‡*Department of Chemistry and Physics, Florida Gulf Coast University, Fort Myers, Florida*

E-mail: dlambrecht@fgcu.edu

Abstract

The adsorption of nitric oxide and nitrogen dioxide (NOx) to the Buckybowls sumanene and corannulene was investigated. Binding energies were up to 1.8x larger than for coronene as the planar analogue, demonstrating the advantages of Buckybowls for gas adsorption. In agreement with previous reports on carbon dioxide and methane adsorption, the favorable binding energies for NOx were shown to be associated with the curvature of the Buckybowls. It is shown that applying an electric field along the bowl symmetry axis modifies the bowl curvatures and impacts adsorbate binding energies, including the potential to desorb adsorbates for repeated use of Buckybowls as adsorbents. As a proof of concept, it is shown that applying electric fields of different strengths and orientations selectively controls sumanene's preference to bind nitric oxide, nitrogen dioxide, and carbon dioxide, suggesting potential applications for dynamically tunable gas adsorption. Moreover, it is demonstrated that adsorbates can be desorbed by applying suitable electric field strengths, allowing to clean the Buckybowls for renewed usage.

Introduction

Gas separation is instrumental for the generation of purified gases and removal of pollutants, such as in the isolation of methane from natural gas or the capture of carbon dioxide from flue gas. Examples of gas separation approaches include membrane filtration,[1–3] cryogenic distillation,[3] absorption,[3,4] and adsorption.[3,5] Recent advances in surface adsorption approaches explored interesting possibilities for tuning the gas selectivity by controlling the surface chemistry.[5] For instance, Guo *et al.* investigated the use of electric fields to modify the adsorption properties of several types of gases on an *h*-BN surface and showed that the strength of the field can be used to induce stronger binding in a reversible interaction with CO_2.[6] Carbon-based materials have also been used for gas capture, such as carbon nanotubes[7–10] and doped graphene sheets.[11–14] Recently, investigations into gas adsorption have

been performed on Buckybowls which can be thought of as molecules derived from Buckyballs (Buckminster fullerene, C_{60}) using a planar cut.[15–20] The curvature of Buckybowls offers favorably strong interaction energies for the binding of small adsorbate molecules, making them promising platforms for gas capture among carbon-based materials. Accordingly, the adsorption of greenhouse gases methane and carbon dioxide on Buckybowls was studied computationally and was found to be more favorable than for coronene as their planar analogue.[17,20] Sumanene was also predicted to be efficient at storing dihydrogen.[21]

This computational study investigates previously unreported interactions of small gas molecules and studies approaches to control the gas adsorption properties of Buckybowls. Specifically, this work quantifies the adsorption interactions of nitric oxide and nitrogen dioxide as relevant gaseous pollutants. Methane and carbon dioxide were also studied as a baseline for comparison to previously published results.[17,20] As a novel angle, gas adsorption to Buckybowls in applied electric fields is studied to explore field impacts on the binding properties. The bowls undergo structural deformation that causes the geometry (such as bowl depth) to change due to the electric field. Our hypothesis was that this change in bowl geometry, combined with polarization of the electron density driven by the applied electric field, alters the adsorption properties such that the selectivity can be tuned for specific gases. Finite electric fields were applied and the adsorbate-adsorbent interactions was studied through density functional theory and energy decomposition analysis (EDA) calculations. For reference, interactions with coronene as the planar analogue of the Buckybowls are presented to compare and identify unique features that arise from the curvature of the molecules.

While this work is a proof of principles study, the test adsorbates are relevant gaseous pollutants. Nitric oxide (NO) and nitrogen dioxide (NO_2) are produced from burning fossil fuels, are toxic to humans, and contribute to chemical processes which create ozone.[22,23] Areas of heavy industry or transportation congestion are impacted by the smog produced from NO, NO_2, and O_3 causing increased occurrence of respiratory illness.[24] Carbon dioxide

and methane are significant green houses gases due to their ability to absorb and re-emit infrared radiation from the surface back towards Earth and have been recorded in increasing concentrations[25,26] due to reasons such as fossil fuel combustion, natural processes, and livestock.[22] While CH_4, CO_2, NO, and NO_2 can be components of a healthy atmosphere, the regulation of these gases is critical to reduce adverse impacts when present in excessive quantities.

This paper is outlined as follows: The computational approaches for calculating the interaction energies (E_{int}), energy decomposition analysis (EDA), and molecular dynamics are briefly outlined. Findings are then presented in the Results and Discussion section which is split into three parts. First, the interactions of gaseous adsorbates with the Buckybowls are analyzed via supermolecular and EDA calculations. Second, the impact of applied electric fields on binding energies is investigated. Third, molecular dynamics results are presented to provide an understanding of the dynamics of the electric-field response. The conclusion summarizes the findings and discusses further avenues of exploration for Buckybowls. Parts of this study have been submitted as part of D.B.'s doctoral thesis.[27]

Computational Approach

The quantum chemistry package Q-Chem[28] was employed to explore the non-covalent adsorbent-adsorbate interactions under the influence of an electric field. Adsorbates were paired with each adsorbent in configurations including both the bowl up (BU) and bowl down (BD) states, where BU is defined as binding to the concave side and BD as binding to the convex side of the Buckybowl (Fig. 1). Together with the one possible binding side for the planar coronene molecule, this resulted in a total of twenty systems to be studied. Several orientations, such as choosing the N or O atom in NO to be closer to the adsorbent, different initial geometries, including positioning the adsorbate over the center, outer ring, and outside of the adsorbent, for each adsorbate were examined by performing a geometry optimization at

the ωB97X-D/pc-1 level of theory. The most stable optimized structures were then used to calculate supermolecular interaction energies with counterpoise correction or energy decomposition analysis (EDA) using an absolutely localized molecular orbital approach at the ωB97M-V/pc-2 level of theory.

The ωB97X-D and ωB97M-V density functionals[29–31] are known to typically reproduce non-covalent interaction energies to within root mean square deviations of 1-2 kcal/mol, providing a balance between speed and accuracy for the prediction of non-covalent interactions.[32] Likewise, the polarization consistent basis sets pc-1 and pc-2 were chosen to balance speed and accuracy in combination with the ωB97-type functionals.[33] The polarization consistent (pc) family of basis sets offers systematic improvement of density functional theory energies at faster basis set convergence than, for example, the well-established correlation consistent basis set family optimized for correlation energies.[33,34] Within this series, pc-1 and pc-2 are basis sets of double- and triple-zeta qualities, respectively. Second-generation energy decomposition analysis (EDA2)[35–38] as implemented within the Q-Chem program package partitions intermolecular interaction energies into a frozen-fragment, polarization, and charge transfer term by casting the wave function into the basis of fragment-localized orbitals and controlling excitations allowed between the fragments: $E_{int} = E_{frz} + E_{pol} + E_{ct}$. The frozen-fragment energy is further divided into an electrostatic, Pauli repulsion, and disperion component: $E_{frz} = E_{el} + E_{Pauli} + E_{disp}$. The electrostatic contribution in EDA2 differs from definitions used in other decomposition approaches such as symmetry-adapted perturbation theory (SAPT) in that EDA2 fragment densities are relaxed to minimize the kinetic energy repulsion. As recommended,[35] we calculate dispersion energies by utilizing ωB97M-V in combination with Hartee-Fock as the dispersionless functional. We found that the EDA2-based dispersion energies are in very good agreement with zero-order symmetry-adapted perturbation theory (SAPT0) results for the systems studied here.

Finite electric fields were applied over a range from -20 to +20 V/nm typically in 0.2 V/nm increments unless otherwise noted. Since practical applications would likely require

the the adsorbent to be attached to a surface, the majority of the field-dependent geometry optimizations presented here utilized an approach where rotations were projected out of the Hessian during optimization under the influence of an electric field. This fixed the field to be parallel to the bowl inversion direction (the symmetry axis of the bowl). We take the bowl symmetry axis to lie along the z-axis so that bowl-up conformations open toward the positive z-direction and bowl-down conformation open toward the negative z-direction. Unless otherwise noted, a positive field direction is defined as the positive pole on below the xy plane and the negative pole above the xy plane.

Results and Discussion

This section analyzes the interaction energies E_{int} between gas molecules and sumanene, corannulene, and coronene. Binding energies were assessed across these systems to compare trends in sensitivities (as indicated by high binding energies) and selectivities (as indicated by differences in binding energies). Moreover, we investigated the effects of applied external electric fields on the binding properties on the Buckybowls and assessed impacts on sensitivity and selectivity. The binding energies were analyzed using the EDA2 method as described above unless otherwise noted.

Trends in binding energies between adsorbates and Buckybowls

In agreement with previously published results,[17,20] adsorption to Buckybowls was found to be stronger in the BU configuration for all adsorbates (Table 1). In general, the interaction energies follow the trend BU sumanene > BU corannulene > coronene > BD sumanene > BD corannulene. One exception is NO_2, where the binding energy to BD corannulene is slightly larger than for BU sumanene, although the difference is well within the error bars of the computational approach. Binding energies to sumanene in BU conformation are typically 2-3 times larger than for BD conformations of identical adsorbates. Interaction

energies with coronene are typically slightly stronger than with sumanene or corannulene in BD conformation but up to 1.8x weaker than in the BU conformations of the Buckybowls. Interestingly, CH_4, CO_2, and NO binding to sumanene in BD conformation is stronger than for corannulene in BD conformation, but binding energies for NO_2 are comparable between BD corannulene and sumanene. Note that the interaction energies for NO and NO_2 on coronene are calculated using supermolecular energies with couterpoise correction in contrast to the other values which are calculated with the EDA2 method. The finding that comparing binding energies for identical adsorbates typically follow the trend BU Buckybowl > coronene > BD Buckybowl suggests that the curvature of the adsorbent plays an important role in binding. This can be rationalized by considering that the BU conformations are able to encapsulate the small adsorbates reported here, creating close adsorbate-adsorbent contacts for favorable binding interactions. The adsorbate-adsorbent contacts increase when switching to the planar coronene and even more so in the bowl-down Buckybowls, thus explaining the weaker binding of adsorbates in this order.

Table 1: Interaction energies in kcal/mol at the ωB97M-V/pc-2 level of theory within the EDA2 approach. [a)] The EDA2 method for NO and NO_2 on coronene failed to converge. Therefore supermolecular interaction energies as obtained at the ωB97M-V/pc-2 level of theory with BSSE corrections are presented.

Molecule	CH_4	CO_2	NO_2	NO
Sumanene (BU)	-5.56	-6.11	-6.04	-4.30
Sumanene (BD)	-1.82	-3.29	-2.33	-2.29
Corannulene (BU)	-4.82	-4.77	-5.19	-3.93
Corannulene (BD)	-1.73	-2.96	-2.35	-2.08
Coronene	-2.95	-3.71	-3.43[a)]	-2.38[a)]

While the structures of CH_4 and CO_2 binding to Buckybowls have been reported previously,[17,20] the results for NO and NO_2 shown in Figure 1 have not been reported before. There are a few important points to note: Nitric oxide is largely oriented parallel to the adsorbent. The oxygen atom points towards the central carbon ring except in the case of corannulene. NO_2 binds to the outer edge in the bowl down cases while it is over the central ring for bowl up. Nitrogen dioxide is positioned horizontally over coronene. With the

exception of the BD configuration of sumanene, the oxygen atoms of NO_2 are oriented away from the bowl in the BU configuration and towards the bowl for BD conformation.

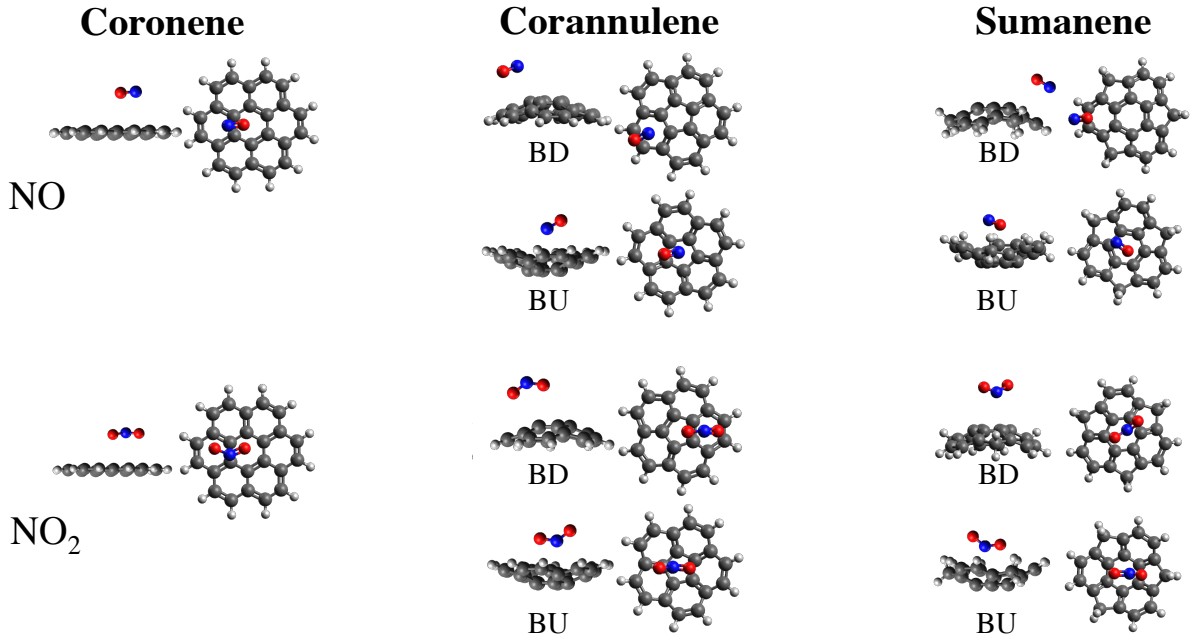

Figure 1: Optimized geometries for NO and NO_2 on coronene, corannulene, and sumanene. Geometries were calculated at the ωB97X-D/pc-1 level of theory. Blue atoms indicates nitrogen while red is oxygen. Configurations where the adsorbate binds to the concave (open) side of the Buckybowl are labeled as "bowl up" (BU), whereas binding to the convex side is denoted "bowl down" (BD).

Binding energy trends within applied electric fields

The comparison of the binding energies to sumanene and corannulene as Buckybowls with the binding energies to coronene as a planar analogue suggests that the curvature of the molecules has a significant impact on adsorbate binding. As has been reported before, the bowl orientation can be flipped by applying an electric field,[39] and our calculations demonstrate that the bowl depth and width can be modified by applying electric fields of different strengths. It is therefore expected that applying electric fields impacts adsorbate binding by influencing the bowl geometry and by driving electronic polarization between the molecules. We tested this hypothesis by studying the absolute and relative strengths of

adsorbate binding to the three adsorbents under applied electric fields.

A few comments about the finite-field calculations are in order before presenting the results. First, it should be noted that the field strengths required in our calculations to induce significant geometry change are likely larger than those previously reported experimentally.[39] One major difference is that the experiment was performed on metal surfaces, which can be expected to have a significant impact on the potential energy surface along the bowl inversion coordinate. Another point is that fairly compact basis sets are needed to yield bound solutions for molecules subjected to electric fields, since ionized solutions are asymptotically more stable in the applied field.[40–43] It should be understood that finite-field bound state calculations are valid only to the extent that the basis set is sufficiently compact to constrain the wave function to the bound solution inside the dissociation barrier. For these reasons, the field strengths reported here should not be interpreted as quantitative predictions but rather as qualitative and proof of concept explorations.

Sumanene

The ordering of the strength of the binding at zero field for sumanene in the BU orientation is NO < CH_4 < NO_2 ≈ CO_2 (Fig. 2). NO is the most weakly bound adsorbate and remains so until 14 V/nm on the positive side and -16 V/nm with a negative field. It is remarkable to note that over the range of -12 to 16 V/nm the total interaction energy of NO remains almost constant in contrast to the behavior exhibited by other adsorbates.

CH_4 displays fairly systematic trends between the applied field strength and the interaction energy. At negative fields, the binding becomes stronger by 2.71 kcal/mol while weakening by 2.05 kcal/mol with a positive field. CO_2 follows similar behavior with smaller changes in interaction energy for positive fields. NO_2 changes the most dramatically with a 2.93 kcal/mol decrease in binding strength with positive applied fields and a 3.31 kcal/mol increase in strength with a negative applied field.

Due to the change in interaction energy of NO_2, the ordering of the binding strengths

change as the field changes. At positive fields, NO_2 becomes more weakly bound than CH_4 so the ordering changes to NO < NO_2 < CH_4 < CO_2. With negative applied fields, NO_2 becomes the most strongly bound at -2 V/nm and the ordering changes to NO < CH_4 < CO_2 < NO_2.

At zero field in the sumanene BD configuration, CO_2 has the strongest interaction energy followed by NO_2 and NO which are nearly the same, and CH_4 with the weakest binding as shown in Figure 2. As a positive electric field is applied, CO_2 remains the most strongly bound until 6 V/nm where the interaction energy of NO_2 becomes comparable. The interaction energy of these two adsorbates initially weakens and then begins to strengthen around 6 V/nm. CH_4 becomes more strongly bound as a positive electric field is applied while NO only becomes weaker. A crossover between CH_4 and NO occurs around 6 V/nm as NO becomes the most weakly bound adsorbate. This behavior suggests that a positive electric field can be used to adjust the selectivity of sumanene toward binding different adsorbates since the ordering of the binding strengths can be controlled. On the other hand, binding becomes stronger across all adsorbates when a negative field is applied. Proceeding toward negative fields, the ordering from zero field is preserved until -8 V/nm when NO becomes the most strongly bound.

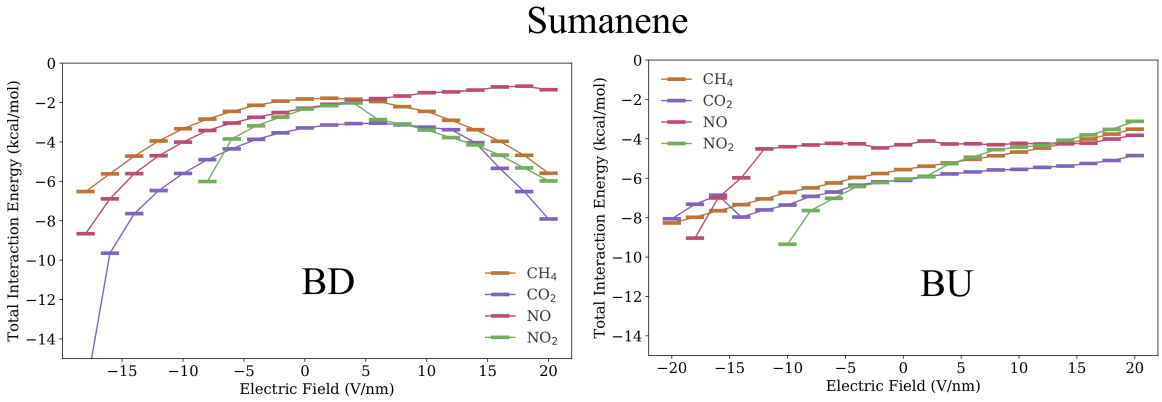

Figure 2: Interactions energies of adsorbates on sumanene as a function of electric field. Bowl down (BD) orientation is shown on the left and bowl up (BU) on the right. Ending lines indicate desorption of the gas molecule at higher field strengths.

Corannulene

At zero field in the corannulene BD configuration, the ordering of binding strengths is CH_4 < NO < NO_2 < CO_2 (Figure 3). With positive applied fields, the interaction energies of NO_2 stay nearly the same with small variations. Similarly, the binding of CH_4 remains nearly constant and becoming slightly more strongly bound at 14 V/nm. NO_2 becomes slightly more strongly bound as positive fields are applied while the binding of CO_2 initially weakens and then becomes slightly stronger. The ordering at positive fields changes to NO < CH_4 < CO_2 < NO_2 at 10 V/nm but the differences in interaction energy are small between NO and CH_4 (0.25 kcal/mol) as well as CO_2 and NO_2 (0.02 kcal/mol). More dramatic changes in interaction energy occur at negative fields where the binding strength increases for each adsorbate. An ordering change occurs at -8 V/nm where NO_2 becomes more strongly bound than CO_2 (CH_4 < NO < CO_2 < NO_2).

In general for the BU systems, interaction strengths become slightly weaker with positive fields while becoming stronger at negative fields. Both NO and CO_2 exhibit only slight changes in interaction energy at positive fields with NO_2 changing the most dramatically. The ordering at zero field (NO < CO_2 < CH_4 < NO_2) is not preserved as it changes to NO < CH_4 < CO_2 < NO_2 at 2 V/nm, NO < CH_4 ≈ NO_2 < CO_2 at 4 V/nm, and then to NO_2 < NO < CH_4 < CO_2 at 6 V/nm. NO_2 changes from being the most strongly bound to the weakest over the course of a 6 V/nm change indicating that the selectivity of NO_2 can be altered using an applied electric field. At negative electric fields a change in the ordering occurs at -6 V/nm (NO < CH_4 < CO_2 < NO_2) where CO_2 becomes more strongly bound than CH_4.

Coronene

Similarly to the BU cases with the Buckybowls, NO has the weakest interaction energy initially for coronene (Figure 4). This trend is preserved at positive fields while a switch in the ordering occurs at -10 V/nm where CH_4 becomes a weaker binding molecule. The

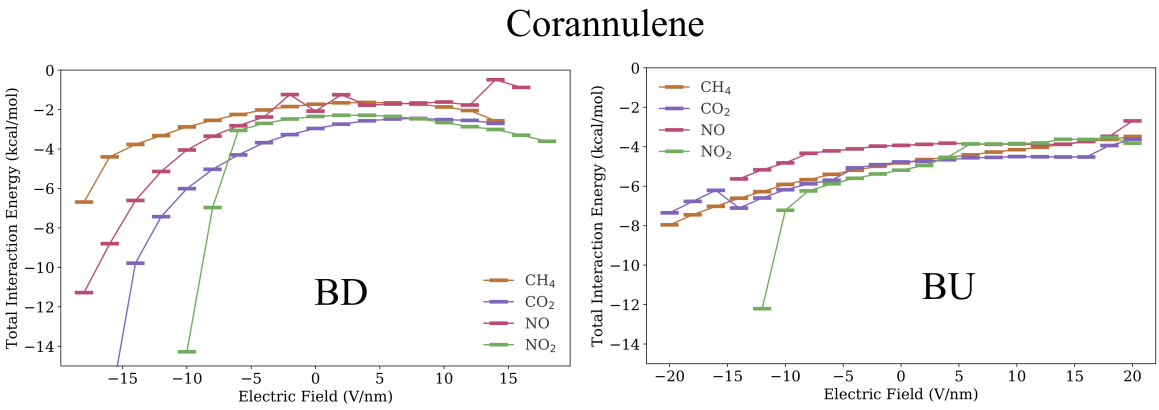

Figure 3: Interactions energies of adsorbates on corannulene as a function of electric field. Bowl down (BD) orientation is shown on the left and bowl up (BU) on the right.

binding energy of NO_2 becomes nearly equivalent to CH_4 at positive fields and shows the same behavior of the binding becoming slightly stronger. At negative fields, NO_2 begins to strongly bind and becomes the strongest at -8 V/nm until it dissociates after -10 V/nm. Overall, the interactions energies either do not change (NO) or become slightly more bound with positive fields where the coronene molecule begins to bend in the BU orientation. Negative fields induce a more precipitous change in the interaction energy as the molecule bends away from the adsorbate in a BD orientation.

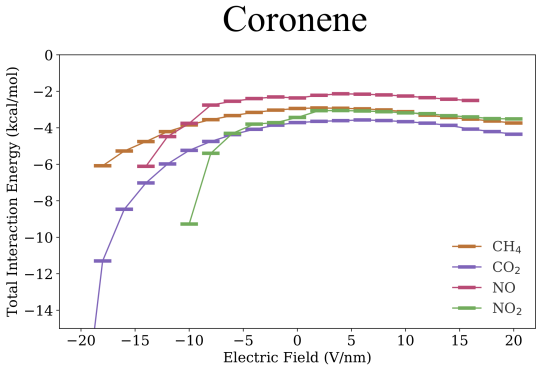

Figure 4: Interactions energies of adsorbates on coronene as a function of electric field. Bowl down (BD) orientation is shown on the left and bowl up (BU) on the right.

Energy decomposition analysis

Energy decomposition analysis was performed to further elucidate the binding mechanisms between the adsorbates and the different adsorbents (Tables S1 through S3). There are three major contributions to the non-covalent interactions between Buckybowls and the studied adsorbates: electrostatics and London dispersion as attractive and Pauli repulsion as repulsive force. In comparison, polarization and charge transfer energies are about an order of magnitude smaller and of only minor impact on the total binding energies. For this reason, we mainly discuss electrostatics, dispersion, and Pauli repulsion in the remainder of this section. However, we note that charge transfer energies have an impact on the trends observed for different field strengths and will therefore be included in sections discussing EDA analysis of field effects.

In general, electrostatic attraction and dispersion forces are strongest in the bowl-up (BU) conformations of the Buckybowls (Tabs. S1 and S2). Electrostatic forces range from -9.00 to -13.95 kcal/mol for NO on corannulene and NO_2 on sumanene in BU conformation, respectively. Dispersion energies range from -7.79 to -10.87 kcal/mol for NO on corannulene and NO_2 on sumanene in BU conformation, respectively. All other electrostatic and dispersion energies for the BU conformations fall within this range.

Electrostatic and dispersion forces are typically smallest in the bowl-down (BD) conformations of the Buckybowls (Tabs. S1 and S2). Electrostatic forces range from -4.82 to -9.59 kcal/mol for CH_4 and NO_2 on corannulene in BD conformation, respectively. Dispersion energies range from -4.23 to -6.28 kcal/mol for CH_4 and NO_2 on corannulene in BD conformation, respectively. All other electrostatic and dispersion energies for the BD conformations fall within this range.

Comparing identical adsorbates, the electrostatic and dispersion energies to coronene are smaller (less attractive) than in the bowl-up conformations of the Buckybowls but larger (more attractive) than in the bowl-down conformations (Tab. S3). Electrostatic energies range from -6.00 to -7.79 kcal/mol for CH_4 and CO_2, respectively. Electrostatic energies

range from -6.15 to -6.58 kcal/mol for the same molecules.

The absolute magnitudes of the Pauli repulsion energies follow similar trends. Repulsion is typically largest for the BU conformations (14.15 to 20.42 kcal/mol) and smallest for BD conformations (7.83 to 14.66 kcal/mol). Comparing identical adsorbates (CH_4 and CO_2), Pauli repulsion energies on coronene again fall in between those for the results for BU and BD Buckybowls (10.03 to 11.62 kcal/kal in coronene versus 7.83 to 10.17 kcal/mol for BD conformations and 14.64 to 18.33 kcal/mol for BU conformations).

These observations on binding energies can be rationalized as follows. The differences in electrostatic binding can be explained by considering that Buckybowls possess electric dipole moments due to the anisotropic distribution of electron density along the bowl symmetry axis. Compared to the planar coronene, excess electron density is found on the outer edge of the bowl creating an electric dipole moment oriented from the bottom of the bowl pointing towards the open end. Binding of an adsorbate in bowl-up conformation (to the concave surface) leads to favorable electrostatic interactions at close distances with the asymmetric electron density of the Buckybowl. In planar coronene, there are fewer close contacts and correspondingly weaker electrostatic interactions. Conversely, adsorbate binding in bowl-down conformation (to the convex surface) leads to the smallest electrostatic interactions due to largest interaction distances. The trends found in the Pauli repulsion energies support this explanation, as the Pauli repulsion indicates penetration of charge densities and therefore the observed trends in the repulsion energies (BU > coronene > BD) suggest that there are more close contacts between absorbate and Buckybowl in BU conformation than there are in adsorbate-coronene interactions, and fewest close contacts in BD conformation.

The trends in London dispersion forces can be explained similarly by considering the geometries of the molecules. Being composed of sections of Buckyballs, Buckybowls possess numerous aromatic carbon rings which contribute to London dispersion interactions. The curvature of the bowls leads to closer contacts for the interactions between adsorbates and the inside of the bowl compared to the outside, explaining the larger dispersion interactions in

BU compared to BD conformation. Interaction distances in coronene are on average shorter than in BD but longer than in BU Buckybowls, explaining that dispersion interactions in coronene are intermediate between those found in BU and BD.

Our findings agree qualitatively with previously published results in that dispersion forces and Pauli repulsion are dominant contributions to the absorbate-Buckybowl binding and are major factors in differentiating adsorption energetics in BU- versus BD-conformations. Specifically, Hussain *et al.* examined non-covalent interactions in coronene, corannulene, and sumanene with CH_4 and CO_2 adsorbates.[20] A localized molecular orbital (LMO) energy decomposition analysis of the interaction energy found that the interactions were largely influenced by the attractive London dispersion force and Pauli repulsion. The magnitudes of these components varied between the bowl up (BU) and bowl down (BD) orientations such that the interactions in the BU case were generally stronger, which agrees qualitatively with the results reported in this work. However, our results also differs from Hussain *et al.* in that we found electrostatic interactions to be of comparable strength as London dispersion. This difference is likely caused by differences in the energy decomposition scheme applied and it will be interesting to further assess similarities and differences between decomposition schemes as applied to Buckybowls in the future.

In the following sections, the EDA results for NO and NO_2 are presented across different electric fields . The results for CH_4 and CO_2 are shown in the supporting information for clarity purposes (Tab. S1 and S2). Additionally, the EDA results for coronene can be found in the SI which includes results for CH_4 and CO_2 (Tab. S3).

Sumanene

As previously mentioned, Figure 2 indicated that an external electric field alters the interaction energy between sumanene and the adsorbates such that the ordering of strengths is changed. NO and NO_2 display clear ordering changes for both the BD and BU cases depending on the applied field strength. In the BD system, positive fields cause the binding

of the two adsorbates to behave differently. While the interaction strength of NO decreases, NO_2 shows an increase in strength. Figure 5 presents the EDA for the NO_x systems to help elucidate the causes for this difference. First, we note an important difference between the zero-field results discussed in the previous section and the comparison of trends across finite fields discussed in this section. While electrostatic, Pauli, and dispersion forces dominate the interaction energies at zero field, charge transfer plays only a minor role in the magnitude of the binding energy at zero field. However, for some systems the changes in electrostatic, Pauli and dispersion energies across different field strengths largely cancel so that the frozen fragment energy (defined as the sum of these components) remains fairly constant across different field strengths. In such cases, the charge transfer energy dominates the trends in binding energies across different field strengths. The frozen fragment interaction contributions are shown in Fig. S2.

By considering the two top graphs in Fig. 5, we note that the change in interaction energy across different field strengths for NO on BD and BU sumanene is largely driven by changes in the charge transfer energy, whereas the frozen fragment energy remains fairly constant throughout. At negative field strengths, the charge transfer energy becomes more attractive while the frozen fragment component becomes slightly repulsive, leading to an overall increased binding at negative field strengths. Whereas the interaction was dominated by the frozen component at zero field, the charge transfer component begins to strengthen and thus compensating for a weaker frozen component. Below -10 V/nm the charge transfer component dominates and leads to a significantly stronger interaction energy. As the field strength is increased, the charge transfer and frozen contributions become weaker until the frozen component begins to be slightly repulsive. Coupled with only a slight increase in the charge transfer component, the total interaction energy becomes weaker at positive field strengths.

The picture for NO_2 is drastically different; its binding energy to sumanene in BD conformation follows trends both in the charge transfer and the frozen fragment energy (bottom

of Fig. 5), where interestingly the frozen fragment contribution dominates at positive field strengths and charge transfer at field strengths below -5 V/nm. NO_2 in the BU configuration exhibits a simple interaction trend of strengthening for negative fields and weakening for positive fields. At zero field the interaction is dominated by the frozen component which largely drives the changes in the interaction energy. The charge transfer component is fairly constant across most field strengths but becomes more apparent at stronger negative fields until desorption occurs below -10 V/nm. The polarization component strengthens slightly for positive fields, but can not compensate for a reduction in the frozen component leading to weaker total interaction energies.

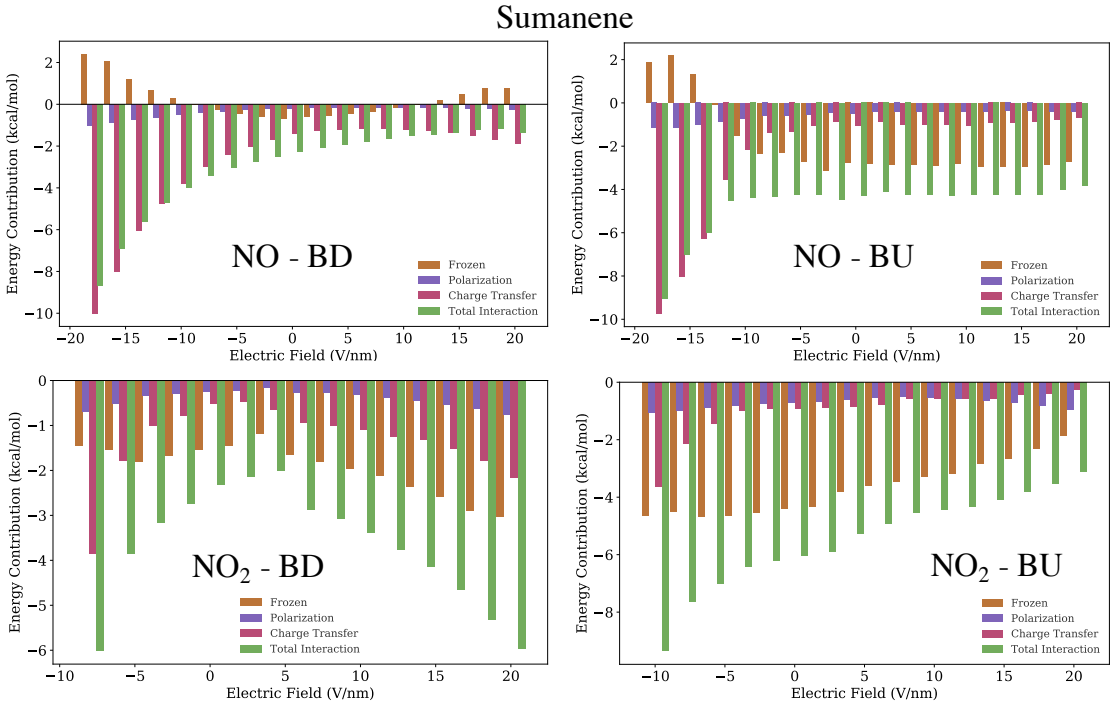

Figure 5: Energy decomposition analysis for NO and NO_2 on sumanene in the bowl down (BD) and bowl up (BU) configurations.

Corannulene

Interaction energies for corannulene show similar trends as those found in the sumanene-based systems with the distinction that the interactions are generally weaker (Fig. 6). In

the BD configurations, NO and NO_2 have similar interaction energies at positive fields with only minor changes as the strength increases before a bowl inversion occurs. Despite these similarities, Figure 6 indicates that the nature of the interactions are somewhat different from those found in sumanene. In the BD conformation, the trends in interaction energies for NO and NO_2 are largely dominated by changes in the charge transfer energy across different strengths. At fields below -10 V/nm, the frozen fragment interaction energies become slightly repulsive, while charge transfer becomes increasingly stabilizing leading to an overall increase in binding energy. We note that NO_2 desorbed at around -10 V/nm in the BD case.

In the BU conformation, the interaction energies for NO and NO_2 have similar values above 6 V/nm, despite the strength of NO_2 binding being stronger than NO by about 1.5 kcal/mol at zero field. The interaction energy of NO does not change much over this range and the EDA as shown in Fig. 6 indicates that the components largely do not change except for a reduction of charge transfer and frozen components above 16 V/nm. Similarly, the EDA components for NO_2 do not change considerably except for a decrease of the charge transfer and frozen components contributing to the reduction in binding energy above 8 V/nm. At negative fields, both systems become more strongly bound due to changes in the charge transfer and polarization component that overcome the reduction of the frozen energy.

Electric field-induced desorption

Applying electric fields to Buckybowls yields the remarkable effect that binding preferences for different adsorbates can be reversed based on the orientations and strengths of the applied fields (Figs. 2-4). Remarkably, we found this tunability to be most pronounced in the BU conformation of sumanene, less so in the BU conformation of corannulene, and only for strong field strengths in the BD conformations and in coronene. This finding suggests that the gas adsorption properties of Buckybowls could be tuned dynamically to match the requirements

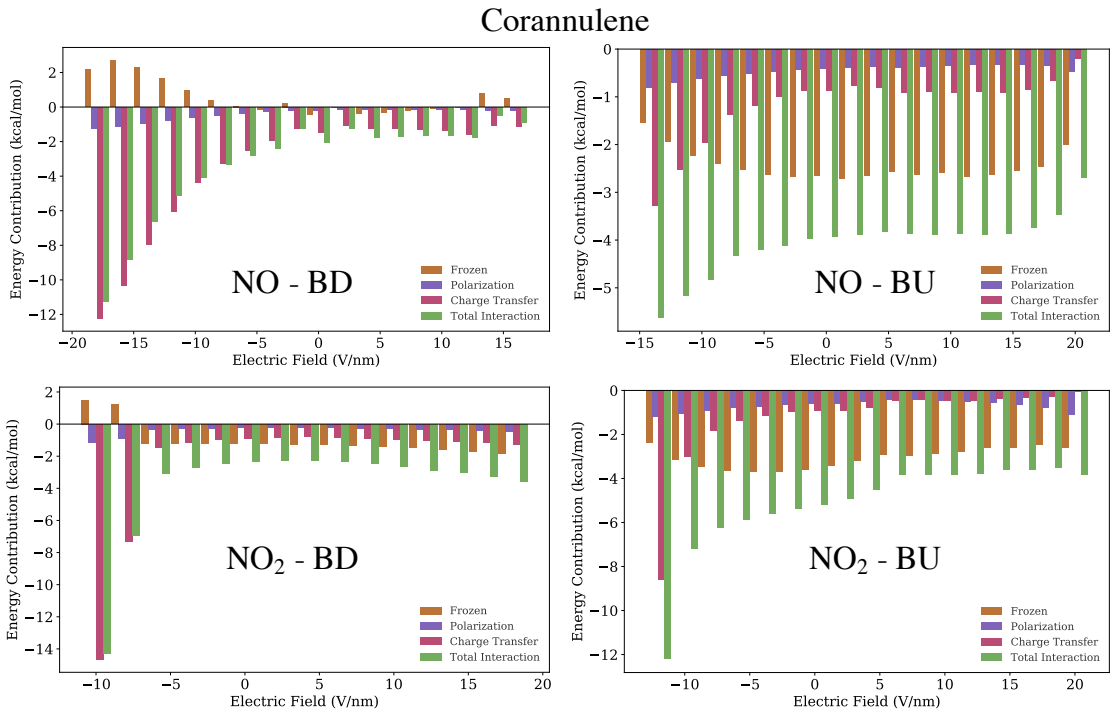

Figure 6: Energy decomposition analysis for NO and NO_2 on corannulene in the bowl down (BD) and bowl up (BU) configurations.

of changing situations. Specifically, the findings described above suggest that electric field stimuli could be employed to induce desorption of adsorbates to clean the Buckybowls for extended use.

To investigate the geometric response of the Buckybowls to applied electric fields and the potential for field-induced desorption, we performed molecular dynamics (MD) simulations of adsorbate-adorbent complexes in applied fields. Fig. 7 shows MD snapshots of the field-induced desorption of NO from sumanene and corannulene, as well as coronene as a reference. In all three cases, the adsorbate detaches after the application of a positive electric field. The time scales for the detachment are of similar magnitudes for all three molecules, ranging from about 100 fs for coronene over 150 fs for sumanene to 250 fs for corannulene for the first visible increase of the intermolecular distance between adsorbate and adsorbent molecules.

To gain a better understanding of the correlation between applied field strength, geometric response, and desorption, we performed geometry optimization studies where we

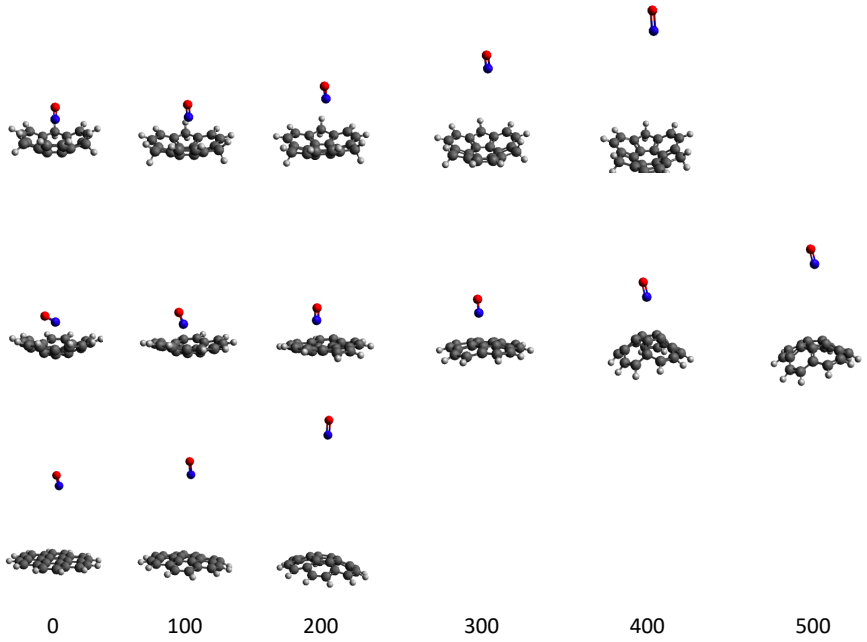

Figure 7: Representative snapshots from electric-field driven molecular dynamics simulations demonstrating the field-induced detachment of NO from sumanene (top), corannulene (middle), and coronene (bottom) at a field strength of $\varepsilon = 0.04$ a.u. (20.6 V/nm). Snapshot numbers are noted below the figure. Simulation temperature was 298 K and step size 0.48 fs.

successively increased the applied field strength in increments of 0.005 a.u. or 2.57 V/nm (Fig. 8). As the field strength increases, the sumanene bowl flattens slightly until at around 12.9 V/nm the adsorbate starts to detach and the bowl starts to deform. At higher field strengths, the bowl inverts. Likewise, corannulene flattens with increasing field strength and undergoes bowl inversion and simultaneous adsorbate detachment at field strengths of 12.9 - 15.4 V/nm. In contrast, coronene shows a deformation from flat to a slight bowl shape as the field strength increases, while the NO detaches at field strengths around 10.3 V/nm.

These findings are noteworthy. Since sumanene and corannulene in BU conformation bind NO up to 1.8x stronger than coronene, one would expect that significantly higher field strengths would be required to release an adsorbate from the Buckybowls than from coronene. However, the Buckybowls release the adsorbate at field strengths comparable to coronene (that is, 20% higher for sumanene). It is conceivable that the unexpectedly low field strengths required for desorption from sumanene and corannulene could be a result of the simultaneous inversion which loosens the binding to the adsorbate.

To better understand the geometric distortion respectively inversion of the corannulene and sumanene molecules in a field, we investigated the potential energy profile along the bowl inversion coordinate via transition state / reaction pathway locating algorithms (Fig. S2). The BU and BD conformation energies are degenerate at zero field. In the applied electric field, this degeneracy is lifted so that in a positive field the bowl-down conformation is favored, explaining the flattening and subsequent inversion of the Buckybowls. We also note that the inversion barrier of 38 kcal/mol in sumanene is significantly higher than that of 14 kcal/mol in corannulene. We also note that the inversion barrier in sumanene remains higher than in corannulene in applied fields, for example 9 kcal/mol and 2 kcal/mol in a field of 10 V/nm, respectively, showing that bowl inversion is more facile in corannulene. These findings explain why we observed more facile bowl inversion for sumanene than for corannulene in Fig. 7.

The inversion barriers in both molecules are reduced in an applied field and the barriers

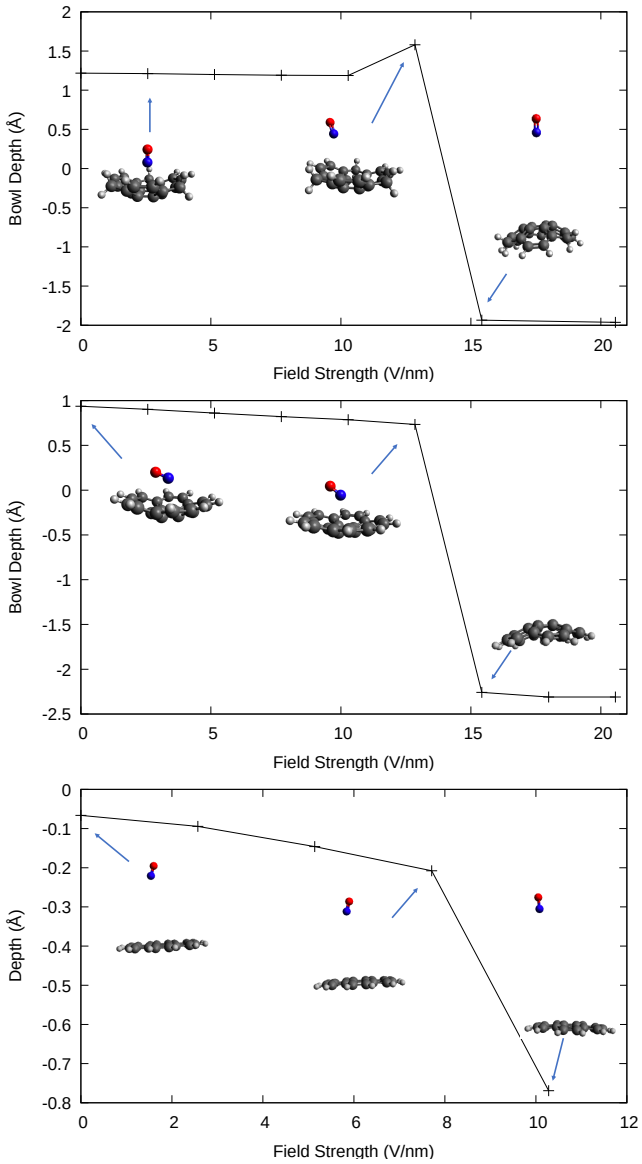

Figure 8: Geometric response and detachment in applied electric fields for NO adsorbed on sumanene (top), corannulene (center), and coronene (bottom). In the rightmost geometry for coronene, the NO has detached and traveled outside the visible frame. The bowl depth is reported as a measure of geometric deformation of the bowl; it is calculated as the distance between the top and bottom carbon atoms relative to the bowl symmetry axis. Positive depths mark bowl-up conformations and negative depths denote bowl-down conformations.

decrease further with higher field strengths. This finding suggests that bowl inversion from bow-up to bowl-down conformation is energetically favored at finite positive field strengths, but bowl inversion is only observed in practice if the barrier has been lowered sufficiently by the applied field. Otherwise the geometry optimization or molecular dynamics simulation may be trapped in the bowl-up conformation as a local minimum. This result explains why the observation of bowl inversion depends on the specifics of the calculation, such as for example starting geometry and increments for field sweeps, since these parameters can impact whether the system is fortuitously trapped in a local minimum or would be found to invert under an applied field.

Turning to studying the desorption mechanism in more detail, we investigated correlations between the detachment process, charge transfer, and molecule-field interaction energies for NO-sumanene. We found that desorption of NO, as measured by the root mean square distance between NO and sumanene, progresses when excess electron density is transferred from sumanene into NO (Fig. 9), leading to negative (positive) charge on NO (sumanene). No detachment is observed without charge transfer between sumanene and NO. This finding suggests an electrostatic explanation for the desorption mechanism. Specifically, the charge separation and increased distance between NO and sumanene enhances the dipole moment of the system, leading to favorable dipole-field interactions that are larger when more charge is transferred and when the charges are separated by a longer distance. This picture explains the driving force for desorption of the NO. This explanation agrees with the observation that the system's total energy decreases with increasing field strength as a result of favorable dipole-field interactions (Fig. S2).

Another interesting question is whether the field effect dominates or whether temperature assists in desorption. To answer this question, we performed molecular dynamics studies of NO on sumanene comparing the desorption at low to moderate temperatures (1 - 400 K) combined with zero and 0.04 a.u. field strengths, respectively (Fig. 10). The findings discussed here are qualitatively similar to those for NO adsorbed on corannulene and coronene

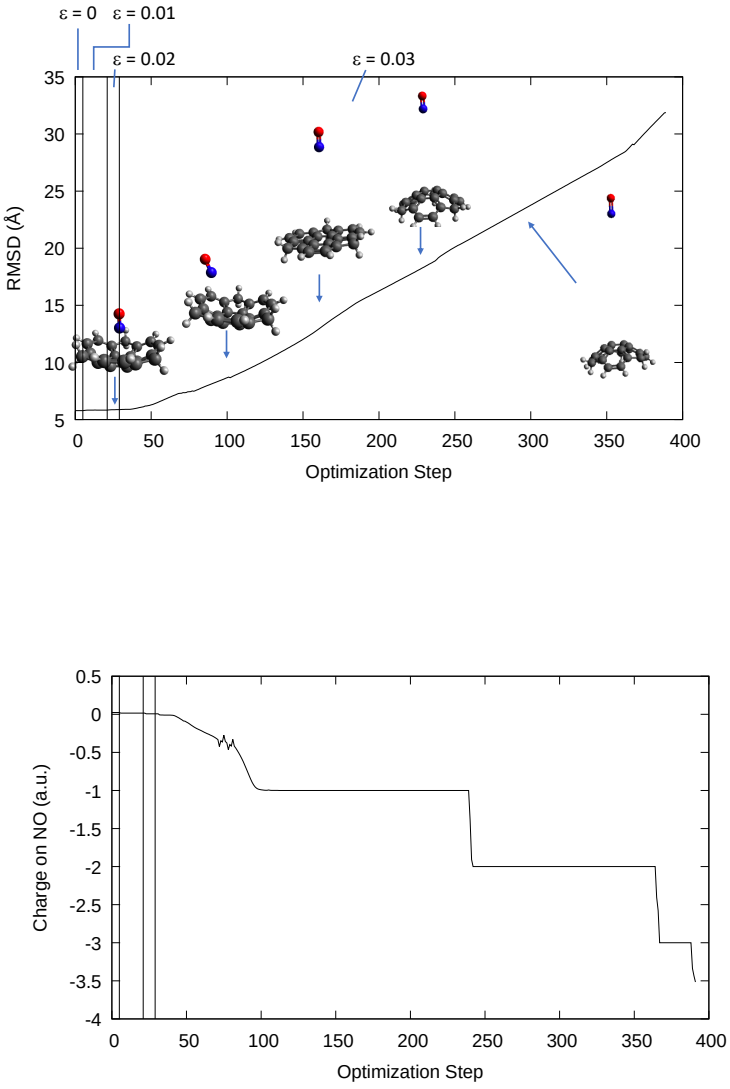

Figure 9: Impact of applying electric fields on the geometry (top) and charge (bottom) of the NO-sumanene complex. Top: Shown are results of geometry optimizations in successively more intense fields; vertical lines denote switches to different field strengths. Bottom: Sum of atomic charges on NO. The geometry and charges change only little up to field strengths of $\varepsilon = 0.02$ a.u. (10.2 V/nm). At a field strength of $\varepsilon = 0.03$ a.u., the sumanene bowl distorts toward a planar geometry during early optimization steps and the bowl inverts at a later optimization step (250). Simultaneously, at this field strength the NO desorbs and continues to move away from the sumanene. The NO-sumanene distance is reported as the root mean square distance (RMSD) between the NO and the sumanene atoms. The applied field cause excess electron density to be transferred into the NO absorbate, as shown by the successively negative charge. Charge transfer and desorption of NO are found to be correlated, as increasing RMSD is connected with increasing excess charge on NO.

(Figs. S11 and S12). Over the time scale studied (approximately 300 fs), temperature and field strength range, we observed field-induced but no temperature-induced desorption. Overall, field-induced desorption is fairly fast with onsets below 300 fs. Interestingly, the onsets exhibit a temperature dependence. At 1 K, the onset of desorption is at about 150 fs. This onset moves to approximately 110 and 90 fs at temperatures of 100 and 200 K, respectively. The earliest onsets of below 50 fs are found at 298 and 400 K, respectively. This data demonstrates that temperature can assist in the desorption process and, as expected, higher temperatures generally lead to easier (earlier) desorption.

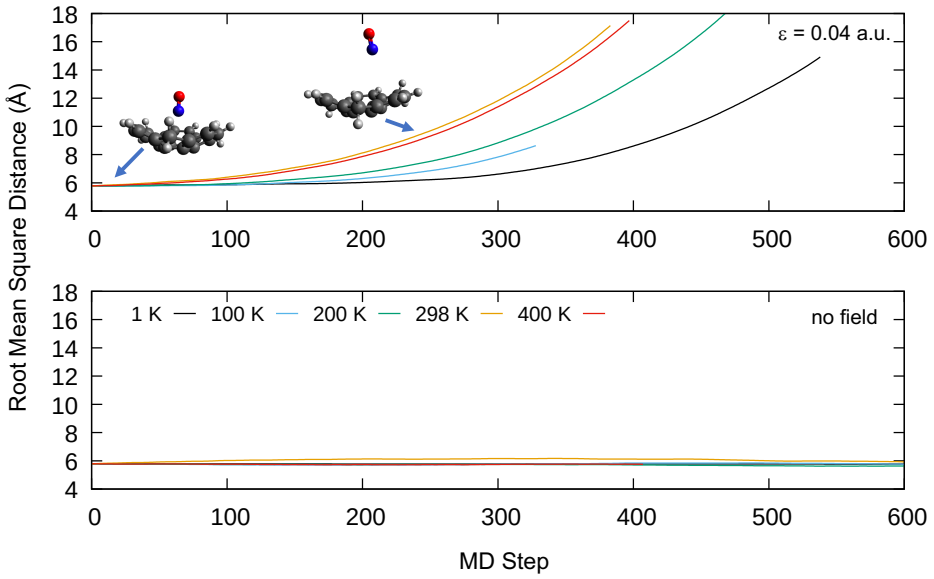

Figure 10: Temperature-dependent molecular dynamics simulation of NO on sumanene. Top: With applied electric field. Bottom: Without field. Shown is the root mean square distance of the adsorbate relative to the Buckybowl.

Conclusion

We presented interaction energies and energy decomposition analyses for CH_4, CO_2, NO, and NO_2 adsorption on Buckybowls. In particular, NO and NO_2 adsorption on Bucky-

bowls has not been previously reported in the literature as far as the authors are aware. We showed that the bowl-up (BU) conformations of sumanene and corannulene bind nitric oxide and nitrogen dioxide about 1.8x stronger than coronene, making Buckybowls more attractive candidates for gas capture and separation compared to their planar analogue. We found that Buckybowls respond to an applied electric field by changing the relative binding preference of adsorbates due to the field-induced deformation of the bowl and charge transfer driven by the field. The concave surface of sumanene shows a particularly strong dependence of adsorbate selectivity to the applied electric field, allowing one to switch the binding preference from CO_2 to NO_2 to NO. We also showed that adsorbates can be removed from the Buckybowls by applying electric fields for repeated usage. This proof of principle study demonstrates the previously unrealized potential of Buckybowls to serve as dynamically tunable gas adsorbents, opening possibilities to develop new capabilities in gas capture and separation. Buckybowls occur in a range of sizes and offer possibilities for chemical modifications, which holds the potential to optimize the binding of specific adsorbates and to enhance the observed response to an applied electric field. Accordingly, we believe that gas adsorption to Buckybowls should be studied more intensively both computationally and experimentally. We expect that Buckybowls will provide form a promising platform for gas separation combining advantages such as favorably high adsorbate binding energies with new capabilities such as dynamically tunable sensitivity and selectivity.

Conflict of interest

There are no conflicts of interest to declare.

Acknowledgement

The authors acknowledge partial support from the National Science Foundation under grant no. CHE-1836552 for the investigation of electric field interactions with Buckybowls. The

authors acknowledge partial support from the Research Corporation for Science Advancement under Cottrell Scholar Award no. 36135 for the investigation of adsorbate binding. This research was supported in part by the University of Pittsburgh Center for Research Computing through the resources provided. D.L. thanks Florida Gulf Coast University for start-up funding. The authors acknowledge useful discussions with Prof. Ken Jordan and Prof. Geoffrey Hutchison and thank Dr. Keith Werling for help with projection of rotations during geometry optimizations in electric fields.

Supporting Information Available

Galleries of optimized structures, binding energies, decomposition analyses, and molecular dynamics results are available in the Supporting Information.

This material is available free of charge via the Internet at `http://pubs.acs.org/`.

References

(1) Baker, R. W. Future directions of membrane gas separation technology. *Industrial & engineering chemistry research* **2002**, *41*, 1393–1411.

(2) Baker, R. W. *Membrane technology and applications*; John Wiley & Sons, 2012.

(3) Wilcox, J. *Carbon capture*; Springer Science & Business Media, 2012.

(4) Budzianowski, W. M. *Energy Efficient Solvents for CO2 Capture by Gas-Liquid Absorption: Compounds, Blends and Advanced Solvent Systems*; Springer, 2016.

(5) Pullumbi, P.; Brandani, F.; Brandani, S. Gas separation by adsorption: technological drivers and opportunities for improvement. *Current Opinion in Chemical Engineering* **2019**, *24*, 131–142.

(6) Guo, H.; Zhang, W.; Lu, N.; Zhuo, Z.; Zeng, X. C.; Wu, X.; Yang, J. CO2 capture on h-BN sheet with high selectivity controlled by external electric field. *The Journal of Physical Chemistry C* **2015**, *119*, 6912–6917.

(7) Valentini, L.; Armentano, I.; Kenny, J.; Cantalini, C.; Lozzi, L.; Santucci, S. Sensors for sub-ppm NO 2 gas detection based on carbon nanotube thin films. *Applied Physics Letters* **2003**, *82*, 961–963.

(8) Santucci, S.; Picozzi, S.; Di Gregorio, F.; Lozzi, L.; Cantalini, C.; Valentini, L.; Kenny, J.; Delley, B. NO 2 and CO gas adsorption on carbon nanotubes: experiment and theory. *The Journal of chemical physics* **2003**, *119*, 10904–10910.

(9) Peng, S.; Cho, K.; Qi, P.; Dai, H. Ab initio study of CNT NO2 gas sensor. *Chemical Physics Letters* **2004**, *387*, 271–276.

(10) Shiraz, H. G.; Astaraei, F. R.; Fardindoost, S.; Hosseini, Z. S. Decorated CNT based on porous silicon for hydrogen gas sensing at room temperature. *RSC Advances* **2016**, *6*, 44410–44414.

(11) Ao, Z.; Yang, J.; Li, S.; Jiang, Q. Enhancement of CO detection in Al doped graphene. *Chemical Physics Letters* **2008**, *461*, 276–279.

(12) Dai, J.; Yuan, J.; Giannozzi, P. Gas adsorption on graphene doped with B, N, Al, and S: a theoretical study. *Applied Physics Letters* **2009**, *95*, 232105.

(13) Kemp, K. C.; Seema, H.; Saleh, M.; Le, N. H.; Mahesh, K.; Chandra, V.; Kim, K. S. Environmental applications using graphene composites: water remediation and gas adsorption. *Nanoscale* **2013**, *5*, 3149–3171.

(14) Sui, Z.-Y.; Meng, Y.-N.; Xiao, P.-W.; Zhao, Z.-Q.; Wei, Z.-X.; Han, B.-H. Nitrogen-doped graphene aerogels as efficient supercapacitor electrodes and gas adsorbents. *ACS applied materials & interfaces* **2015**, *7*, 1431–1438.

(15) Armaković, S.; Armaković, S. J.; Šetrajčić, J. P. Hydrogen storage properties of sumanene. *international journal of hydrogen energy* **2013**, *38*, 12190–12198.

(16) Jaafar, R.; Pignedoli, C. A.; Bussi, G.; Ait-Mansour, K.; Groening, O.; Amaya, T.; Hirao, T.; Fasel, R.; Ruffieux, P. Bowl inversion of surface-adsorbed sumanene. *Journal of the American Chemical Society* **2014**, *136*, 13666–13671.

(17) Armaković, S.; Armaković, S. J.; Šetrajčić, J. P.; Jaćimovski, S. K.; Holodkov, V. Sumanene and its adsorption properties towards CO, CO 2 and NH 3 molecules. *Journal of molecular modeling* **2014**, *20*, 2170.

(18) Armaković, S.; Armaković, S. J.; Pelemiš, S.; Mirjanić, D. Influence of sumanene modifications with boron and nitrogen atoms to its hydrogen adsorption properties. *Physical Chemistry Chemical Physics* **2016**, *18*, 2859–2870.

(19) Reisi-Vanani, A.; Mehrdoust, S. Effect of boron doping in sumanene frame toward hydrogen physisorption: A theoretical study. *International Journal of Hydrogen Energy* **2016**, *41*, 15254–15265.

(20) Hussain, M. A.; Vijay, D.; Sastry, G. N. Buckybowls as adsorbents for CO2, CH4, and C2H2: Binding and structural insights from computational study. *Journal of computational chemistry* **2016**, *37*, 366–377.

(21) Della, T. D.; Suresh, C. H. Sumanene: an efficient π-bowl for dihydrogen storage. *Physical Chemistry Chemical Physics* **2018**, *20*, 6227–6235.

(22) Hockstad, L.; Hanel, L. *Inventory of US greenhouse gas emissions and sinks*; 2018.

(23) Seinfeld, J. H.; Pandis, S. N. *Atmospheric chemistry and physics: from air pollution to climate change*; John Wiley & Sons, 2016.

(24) Price, D.; Birnbaum, R.; Batiuk, R.; McCullough, M.; Smith, R. *Nitrogen oxides: Impacts on public health and the environment*; 1997.

(25) Dlugokencky, E. Global CO_2 Monthly Means. https://www.esrl.noaa.gov/gmd/ccgg/trends/gl_data.html, NOAA/ESRL.

(26) Dlugokencky, E. Global CH_4 Monthly Means. https://www.esrl.noaa.gov/gmd/ccgg/trends_ch4/, NOAA/ESRL.

(27) Burrill, D. J. Ab InitioInvestigations of Gas Adsorption on Buckybowls. Ph.D. thesis, University of Pittsburgh, 2020.

(28) Shao, Y.; Gan, Z.; Epifanovsky, E.; Gilbert, A. T.; Wormit, M.; Kussmann, J.; Lange, A. W.; Behn, A.; Deng, J.; Feng, X. et al. Advances in molecular quantum chemistry contained in the Q-Chem 4 program package. *Molecular Physics* **2015**, *113*, 184–215.

(29) Chai, J.-D.; Head-Gordon, M. Long-range corrected hybrid density functionals with damped atomatom dispersion corrections. *Physical Chemistry Chemical Physics* **2008**, *10*, 6615.

(30) Mardirossian, N.; Head-Gordon, M. Mapping the genome of meta-generalized gradient approximation density functionals: The search for B97M-V. *The Journal of chemical physics* **2015**, *142*, 074111.

(31) Mardirossian, N.; Head-Gordon, M. ωB97M-V: A combinatorially optimized, range-separated hybrid, meta-GGA density functional with VV10 nonlocal correlation. *Journal of Chemical Physics* **2016**, *144*, 214110.

(32) Mardirossian, N.; Head-Gordon, M. Thirty years of density functional theory in computational chemistry: An overview and extensive assessment of 200 density functionals. *Molecular Physics* **2017**, *115*, 2315–2372.

(33) Jensen, F. Polarization consistent basis sets: Principles. *J. Chem. Phys.* **2001**, *115*, 9113.

(34) Thom H. Dunning, J. Gaussian basis sets for use in correlated molecular calculations. I. The atoms boron through neon and hydrogen. *J. Chem. Phys.* **1989**, *90*, 1007.

(35) Horn, P. R.; Mao, Y.; Head-Gordon, M. Probing non-covalent interactions with a second generation energy decomposition analysis using absolutely localized molecular orbitals. *Phys. Chem. Chem. Phys.* **2016**, *18*, 23067–23079.

(36) Horn, P. R.; Head-Gordon, M. Alternative definitions of the frozen energy in energy decomposition analysis of density functional theory calculations. *The Journal of Chemical Physics* **2016**, *144*, 084118.

(37) Horn, P. R.; Mao, Y.; Head-Gordon, M. Probing non-covalent interactions with a second generation energy decomposition analysis using absolutely localized molecular orbitals. *Physical Chemistry Chemical Physics* **2016**, *18*, 23067–23079.

(38) Horn, P. R.; Head-Gordon, M. Alternative definitions of the frozen energy in energy decomposition analysis of density functional theory calculations. *Journal of Chemical Physics* **2016**, *144*, 084118.

(39) Fujii, S.; Ziatdinov, M.; Higashibayashi, S.; Sakurai, H.; Kiguchi, M. Bowl Inversion and Electronic Switching of Buckybowls on Gold. *Journal of the American Chemical Society* **2016**, *138*, 12142–12149.

(40) Yamabe, T.; Tachibana, A.; Silverstone, H. J. Theory of the ionization of the hydrogen atom by an external electrostatic field. *Phys. Rev. A* **1977**, *16*, 877890.

(41) Lanczos, C. Zur Intensittsschwächung der Spektrallinien in hohen elektrischen Feldern. *Zeitschrift für Physik* **1931**, *68*, 204–232.

(42) Lanczos, C. Zur Theorie des Starkeffekts in hohen Feldern. *Zeitschrift für Physik* **1930**, *62*, 518–544.

(43) Lanczos, C. Zur Verschiebung der Wasserstoffterme in hohen elektrischen Feldern. *Zeitschrift für Physik* **1930**, *65*, 431–455.

Graphical TOC Entry